



Synthesis, Structure and Thermal Analysis of Silver Nanoparticles using Bakelite Composite

GIRIRAJ TAILOR¹, SARVESH KUMAR SHAILESH^{2,*}, JYOTI CHAUDHARY¹ and SUHAIL AFZAL²

¹Polymer Science Laboratory, Department of Chemistry, Mohanlal Sukhadia University, Udaipur-313 001, India

²Department of Chemistry, Baddi University of Emerging Science and Technology, Baddi-173 205, India

*Corresponding author: E-mail: skshailesh07@gmail.com

Received: 9 June 2017;

Accepted: 17 August 2017;

Published online: 31 January 2018;

AJC-18728

In present work, silver nanoparticles are synthesized using phenol and formaldehyde by chemical precipitation method. To obtain the silver nanoparticles, synthesized bakelite complex is decomposed at the 1100 °C. The formation of the synthesized bakelite composite is confirmed by the infra-red spectroscopy and nuclear magnetic resonance spectroscopy. The chemical composition and crystallographic structure of silver nanoparticles are confirmed by XRD, while scanning electron microscopy and atomic force microscopy are used to characterize the morphology of nanoparticles as well as the distribution of nanoparticle in composite. The SEM analysis indicates the ductile and catastrophic brittle fracture present on the surface of the nanoparticles. The XRD analysis revealed the size of the nanoparticle and the crystal structure which are 24 nm and orthorhombic, respectively. Thermogravimetric analysis determined the 68 % stability of compound at 900 °C and the process being endothermic.

Keywords: Bakelite, Catastrophic brittle, Silver nanoparticles, Orthorhombic.

INTRODUCTION

The synthesis of nanoparticles is a rapidly growing field in the material science [1]. Metal nanoparticles are particularly interesting because they can easily be synthesized, modified chemically and can be suitably applied for device fabrication [2-4]. A variety of method have been developed for the preparation of metallic nanoparticles [5,6] like reverse micelles process [6,7], salt reduction [8], microwave dielectric heating reduction [9], ultrasonic irradiation [10], radiolysis [11,12], solvothermal synthesis [13], electrochemical synthesis [13,14], etc. Due to the specific size, shape and distribution, nanoparticles are used in the production of novel material such as sensors [15], resonators [16], actuators [17] reactors [18], single electron tunneling devices [19] and plasmonics [20], etc.

The noble metal nanoparticles have attracted much attention due to their unique physical, electronic, optical, mechanical and magnetic properties that are significantly different from those of bulk materials [21]. These special and unique properties could be attributed to their small sizes and very large specific surface area. In recent years, a lot of researches focused on silver nanoparticles because of their important scientific and technological applications in photosensitive components [22,23], photocatalyst [24], sensors [25,26] and especially in surface enhanced Raman scattering [27,28]. Such properties and applications strongly depend on the morphology, crystal

structure, stress, strain, toughness, rigidity, joint, crack and dimensions of silver nanostructures. In past years, silver thin films have been a subject of interest for researchers because of excellent optical, electrical, catalytic, sensing and antimicrobial properties [29,30] and subsequent applications.

In this article, the synthesis of silver nanoparticles is performed by using phenol and formaldehyde using chemical precipitation method. The prepared bakelite composite have been examined using infrared spectroscopy and nuclear magnetic spectroscopy. The silver nanoparticles are synthesized by the decomposition of bakelite composite at 1100 °C and its characterization is performed by using X-ray diffraction, scanning electron microscope, atomic force microscopy and thermogravimetric analyses.

EXPERIMENTAL

All the chemicals used were of analytical reagent grade. These are used without any purification. Phenol and formaldehyde are obtained from Central Drug House and silver nitrate is purchased from Qualikems.

The functionalization test of bakelite composite material is performed by IR and NMR spectroscopy. The morphology and crystal structure of silver nanoparticles powder is evaluated by SEM and XRD. SEM images are obtained using a field emission scanning electron microscope (Zeiss EVO 18 Germany) at an accelerating voltage of 15 KV. The reaction type and weight loss is confirmed using TGA/DTA thermal system (DTG-60, Shimadzu,

Kyoto, Japan). The XRD pattern is recorded by X-ray diffractometer (PAN Analytical X'Pert, Almelo, The Netherlands) equipped with Ni filter and $\text{CuK}\alpha$ ($\lambda = 1.54056 \text{ \AA}$) radiation source.

Synthesis of silver-bakelite composite: Silver nitrate (1 N) solution was treated with phenol, formaldehyde and conc. HCl. The mixture was heated for 30 min. The dried solid sample was washed with distilled water in order to remove the excess metal ions and impurities.

Synthesis of silver nanomaterials: In order to obtain silver nanoparticles, silver-bakelite composite is decomposed by heating at $1100 \text{ }^\circ\text{C}$ for 1 h.

RESULTS AND DISCUSSION

In IR spectra, O-H stretching vibration is indicated at the broad peak at 3520 cm^{-1} . C-H stretching low signal bakelite occurs at $3153\text{--}3128 \text{ cm}^{-1}$. The strong intense band at 2353 cm^{-1} of silver-bakelite composite can be attributed to C-H stretching in CH_2 . The band at 1600 cm^{-1} assigned to C=O stretching present in the silver-bakelite composite with hydrogen bonding. The sharp band at 1332 cm^{-1} can be assigned to O-H bending in silver-bakelite composite (Fig. 1).

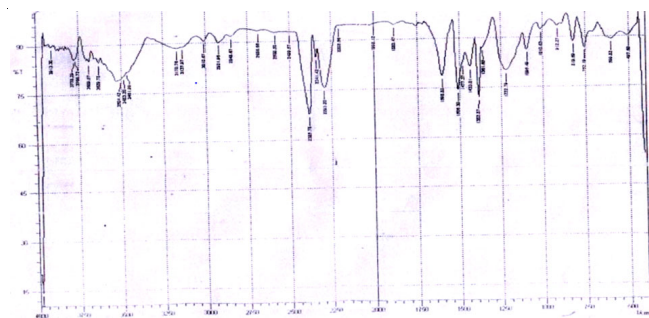


Fig. 1. IR spectra of synthesized bakelite composite

In $^1\text{H NMR}$ spectra of the synthesized composite, phenolic protons were observed with chemical shifts within the range 3.524 ppm (Fig. 2). In this spectra, signal with chemical shift at 2.471 ppm represents benzylic proton in the complex. The chemical shift at 6.744 ppm represent the aromatic protons in bakelite complex.

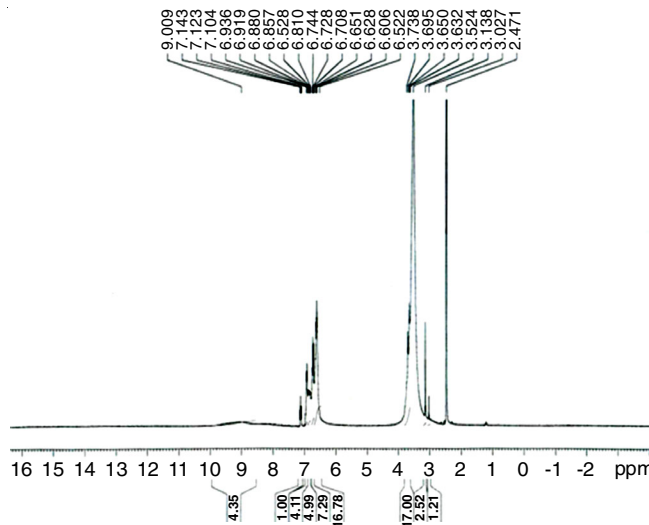


Fig. 2. NMR spectra of synthesized bakelite composite

In SEM micrographs, the grey coloured regions indicate the bulk polymer matrix and the brighter spots indicate the distribution of silver particles. The cross-sectional area is smooth and dense, without any evidence of pores or channels. On the other hand, the surface is completely rough due to the homogeneous distribution of silver metal particle aggregated at polymer surface. This could be attributed to the chemical interactions between the polar silver metal particle on surface and polar bonds present in the segments of phenol-formaldehyde. This analyses also confirmed the ductile and brittle type. It described that the amount of nanoscale plastic deformation on the surface that precedes fracture. The presence of catastrophic brittle fracture occurs due to the elastic stress which is present on the surface and usually propagates at high speed. Fracture occurring in a brittle manner is neither anticipated by the onset of prior macro-scale visible permanent distortion to cause shut down of operating equipment, nor it can be arrested by a removal of the load except for very special circumstances. It must be pointed out that ductile and brittle can also be applied to fracture on a microscopic level.

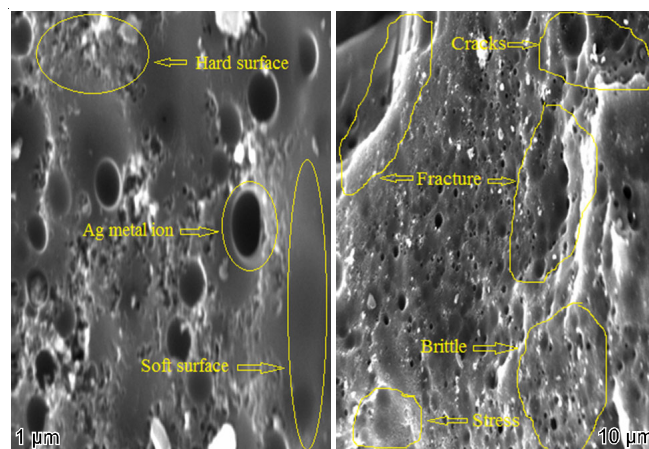


Fig. 3. SEM image of silver nanoparticles synthesized by the decomposition of bakelite composite

The possible nanostructure features is associated with the basic types of external load conditions *e.g.*, overload, fatigue, and environmentally assisted sustained load cracking. As indicated in the morphology, dimpled fracture surface is uniquely associated with the nanoscale mechanism of nano void coalescence, which is further associated with macroscopic ductile fractures. However, limiting the plastic deformation to a small volume of material can also cause brittle fractures, while the fracture process is still micro void coalescence. This case represents the constraining of ductile fracture mechanism of micro void coalescence to a plain strain, strain fracture mode referred to as plane-strain micro void coalescence or occurs preferentially in the limited region adjacent to grain boundary resulting in a dimpled intergranular fracture surface. Silver metallic material fracture surfaces showing large fractions of cleavage may show cracking on more than one crystallographic plane within a given grain, leading to the most common feature associated with brittle faceted fracture [31,32].

Surface imaging studies were performed using atomic force microscopy (AFM) for estimating surface morphology and particle size distribution. By this investigation, the linear den-

driftic shape of metal ions presents at the surface of silver nanoparticle is identified. The white spots in Fig. 4 show the presence of silver metal ions in rare linear dendritic form. The particle size predicted is 32 nm in length and the maximum peak height obtained is of 179.25 nm with no peaks in between [33]. The distance between peak to peak in y-direction is 179 nm and in z-direction is 89.78 nm. Average sizes of peaks are 101.38 nm or defined line distanced from the mean line (z_i) with roughness approximately 20.93 nm, which can be calculated as follows:

$$R_a = \frac{1}{L} \int_0^L [z(x)] dx$$

where $z(x)$ is the function that describes the surface profile analyzed in terms of height (z) and position (x) of the sample over the evaluation length "L" [34-36]. The second moment of material is calculated to be 104.649 nm. Root mean square of mean profile slope is found to be 25.94 nm at different counts (N).

$$R_q = \sqrt{\frac{1}{N-1} \sum_{i=1}^{N-1} \left(\frac{\partial z_i}{\partial x_i} - \frac{1}{N-1} \sum_{i=1}^{N-1} \left(\frac{z_i - z_{i-1}}{x_i - x_{i-1}} \right) \right)^2}$$

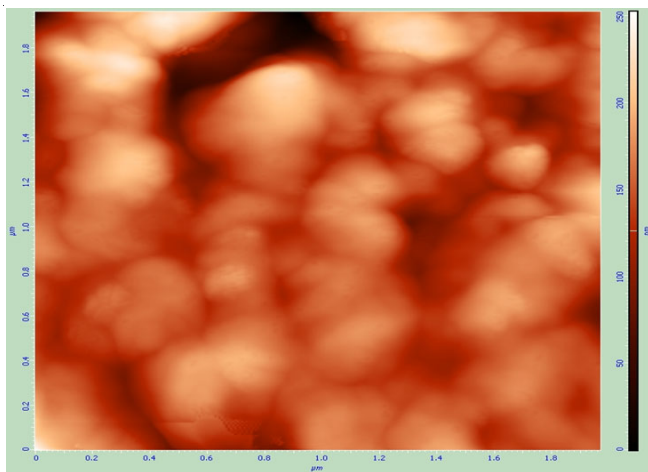


Fig. 4. AFM image of silver nanoparticles

Surface skewness which is the third moment of profile amplitude probability density functions found to be of range -0.1049. Negative sign shows that surface is more planar and valleys are predominant. Coefficient of kurtosis is -0.1521 which shows mesocratic surface as the value is less than 3. From Fig. 5, it has been observed that number of peaks crossing above the upper threshold and below the lower threshold per length of trace in a profile is in between 20-100 peak count for 60-160 nm bandwidth range.

X-ray diffraction: X-ray diffraction pattern stipulates an effective method for determining the phase and crystallite size of silver nanoparticles. The diffraction peaks in each XRD pattern can be assigned to reflections from the (020), (001), (111), (121), (200), (131) and (211) planes of the orthorhombic silver nanoparticles (Fig. 6). The broad peaks in the XRD pattern indicate that the silver nanoparticles are small [36]. X-ray diffraction pattern also indicates that with increase in the annealing temperature from 50 to 200 °C, there is no any effective change in XRD peak intensity, while in between 350

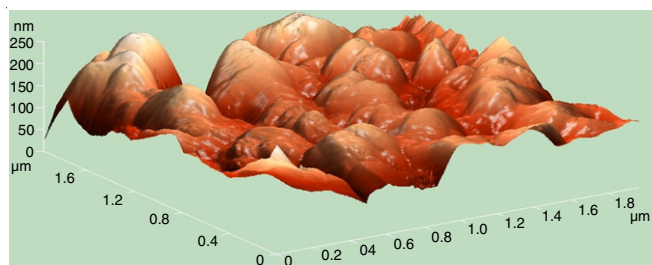


Fig. 5. 3D image of silver nanoparticles

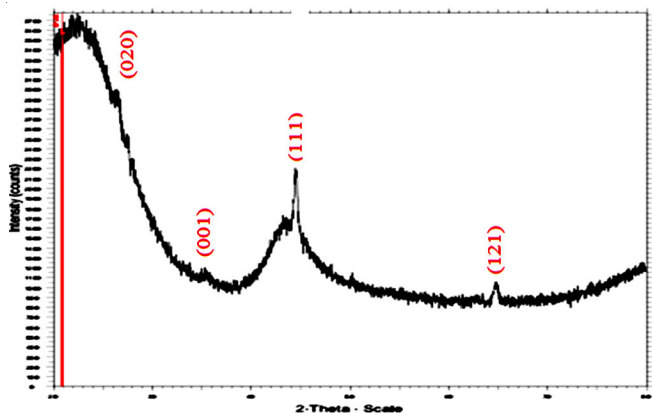


Fig. 6. XRD graph of silver nanoparticles

and 500 °C, all the peaks of hexagonal phase are well resolved and their peak intensity also increases, indicating increased crystallinity of the corresponding silver nanoparticles [37]. To determine the crystallinity, the ratio of intensity at the peaks (111) and (121) is calculated at 2θ values 44 and 64 and assumed it as 100 % crystalline for reference [38]. With the above as reference, the crystallinity percentage is found to be 76 % which confirms the improvement in crystallinity when annealing temperature is raised. The growths in crystalline size as well as reduction in full width at half maxima (FWHM) of XRD peak are also observed on increasing the annealing temperature. The calculated lattice constants are found to be $a = 10.43$ nm, $b = 22.35$ and $c = 7.98$ nm for the above orthogonal samples. The ratio of lattice constants $a/b = 0.46667$ and $c/b = 0.35705$ confirms the orthogonal structures of silver nanoparticles [39].

Thermal analysis: In TGA thermogram (Fig. 7) predicted 32 % mass decomposition of metal ion in silver nanoparticles from 21-900 °C [40,41]. A heating up to 100 °C/min, there is few loss in weight sample with the increase temperature. The decomposition of bakelite complex took place at a slower rate of 1.265 % loss in weight per 29 °C increase in temperature up to 100 °C.

Conclusion

In this work, bakelite composite was synthesised from phenol and formaldehyde using chemical precipitation method, which in turn by decomposing the composite, silver nanoparticles were synthesized at 1100 °C. The prepared bakelite composite have been examined using infrared spectroscopy and nuclear magnetic spectroscopy. The atomic force microscopy is used to estimate the surface morphology and particle size, and the linear dendritic shape of silver ions presents at

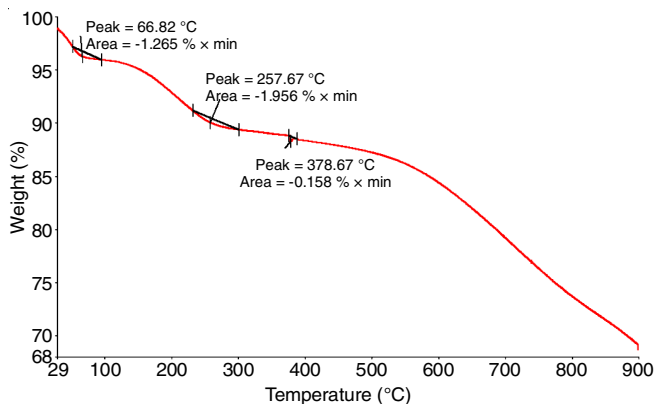


Fig. 7. TGA graph of silver nanoparticles

the surface of nanoparticles, which can be of great advantages for drug delivering or chemical catalytic reactions in controlled and efficient manner. The SEM analysis ascertains the completely rough surface due to the homogeneous distribution of the silver metal particles accumulated at the polymer surface. The XRD analysis revealed that crystal structure is orthorhombic and growth in crystallite size as well as reduction in full width at half maxima (FWHM) at the peak are also observed on increasing the annealing temperature.

ACKNOWLEDGEMENTS

The authors are thankful to IIT Jodhpur and Rajasthan University, Jaipur, India for characterization of nanoparticles and providing the spectral and analytical facilities.

REFERENCES

- C. Petit, P. Lixon and M.P. Pileni, *J. Phys. Chem.*, **97**, 12974 (1993); <https://doi.org/10.1021/j100151a054>.
- C.P. Collier, R.J. Saykally, J.J. Shiang, S.E. Henrichs and J.R. Heat, *Science*, **277**, 1978 (1997); <https://doi.org/10.1126/science.277.5334.1978>.
- P.L. McEuen, D.L. Klein, R. Roth, A.K.L. Lim and A.P. Alivisatos, *Nature*, **389**, 699 (1997); <https://doi.org/10.1038/39535>.
- M. Sastry, A. Gole and S.R. Sainkar, *Langmuir*, **16**, 3553 (2000); <https://doi.org/10.1021/la990948a>.
- A. Pal, S. Shah and S. Devi, *Colloids Surf. A*, **302**, 483 (2007); <https://doi.org/10.1016/j.colsurfa.2007.03.032>.
- M.J. Rosemary and T. Pradeep, *Colloids Surf. A*, **268**, 81 (2003); <https://doi.org/10.1016/j.jcis.2003.08.009>.
- Y. Xie, R. Ye and H. Liu, *Colloids Surf. A*, **279**, 175 (2006); <https://doi.org/10.1016/j.colsurfa.2005.12.056>.
- M. Maillard, S. Giorgio and M.-P. Pileni, *Adv. Mater.*, **14**, 1084 (2002); [https://doi.org/10.1002/1521-4095\(20020805\)14:15<1084::AID-ADMA1084>3.0.CO;2-L](https://doi.org/10.1002/1521-4095(20020805)14:15<1084::AID-ADMA1084>3.0.CO;2-L).
- Z.S. Pillai and P.V. Kamat, *J. Phys. Chem. B*, **108**, 945 (2004); <https://doi.org/10.1021/jp037018r>.
- K. Patel, S. Kapoor, D.P. Dave and T. Mukherjee, *Chem. Sci.*, **117**, 53 (2005); <https://doi.org/10.1007/BF02704361>.
- R.A. Salkar, P. Jeevanandam, S.T. Aruna, Y. Kolytipin and A. Gedanken, *J. Mater. Chem.*, **9**, 1333 (1999); <https://doi.org/10.1039/a900568d>.
- B. Soroushian, I. Lampre, J. Belloni and M. Mostafavi, *Radiat. Phys. Chem.*, **72**, 111 (2005); <https://doi.org/10.1016/j.radphyschem.2004.02.009>.
- M. Starowicz, B. Stypula and J. Banac, *Electrochem. Commun.*, **8**, 227 (2006); <https://doi.org/10.1016/j.elecom.2005.11.018>.
- J.-J. Zhu, X.-H. Liao, X.-N. Zhao and H.-Y. Chen, *Mater. Lett.*, **49**, 91 (2001); [https://doi.org/10.1016/S0167-577X\(00\)00349-9](https://doi.org/10.1016/S0167-577X(00)00349-9).
- S. Liu, W. Huang, S. Chen, S. Avivi and A. Gedanken, *J. Non-Cryst. Solids*, **283**, 231 (2001); [https://doi.org/10.1016/S0022-3093\(01\)00362-3](https://doi.org/10.1016/S0022-3093(01)00362-3).
- K.L. Ekinci, X.H. Huang and M.L. Roukes, *Appl. Phys. Lett.*, **84**, 4469 (2004); <https://doi.org/10.1063/1.1755417>.
- W.C. Lee and Y.H. Cho, *Curr. Appl. Phys.*, **7**, 139 (2007); <https://doi.org/10.1016/j.cap.2006.03.001>.
- C. Roos, M. Schmidt, J. Ebenhoch, F. Baumann, B. Deubzer and J. Weis, *Adv. Mater.*, **11**, 761 (1999); [https://doi.org/10.1002/\(SICI\)1521-4095\(199906\)11:9<761::AID-ADMA761>3.0.CO;2-D](https://doi.org/10.1002/(SICI)1521-4095(199906)11:9<761::AID-ADMA761>3.0.CO;2-D).
- S.H. Hong, H.K. Kim, K.H. Cho, S.W. Hwang, J.S. Hwang and D. Ahn, *J. Vac. Sci. Technol. B*, **24**, 136 (2006); <https://doi.org/10.1116/1.2150227>.
- J.R. Krenn, J.C. Weeber, A. Dereux, E. Bourillot, J.P. Goudonnet, G. Schider, A.R. Leitner, F. Aussenegg and C. Girard, *Phys. Rev. B*, **60**, 5029 (1999); <https://doi.org/10.1103/PhysRevB.60.5029>.
- M. Mazur, *Electrochem. Commun.*, **6**, 400 (2004); <https://doi.org/10.1016/j.elecom.2004.02.011>.
- A. Biswas, O.C. Aktas, U. Schurmann, U. Saeed, V. Zaporozhtchenko, F. Faupel and T. Strunskus, *Appl. Phys. Lett.*, **84**, 2655 (2004); <https://doi.org/10.1063/1.1697626>.
- M. Quinten, *Appl. Phys. B*, **73**, 317 (2001); <https://doi.org/10.1007/s003400100666>.
- G.I. Stegeman and E.M. Wright, *Opt. Quantum Electron.*, **22**, 95 (1990); <https://doi.org/10.1007/BF02189947>.
- A. Biswas, H. Eilers, F. Hidden Jr., O.C. Aktas and C.V.S. Kiran, *Appl. Phys. Lett.*, **88**, 13103 (2006); <https://doi.org/10.1063/1.2161401>.
- H. Wei and H. Eilers, *J. Phys. Chem. Solids*, **70**, 459 (2009); <https://doi.org/10.1016/j.jpcs.2008.11.012>.
- C.E. Talley, J.B. Jackson, C. Oubre, N.K. Grady, C. Hollars, S.M. Lane, T.R. Huser, P. Nordlander and N.J. Halas, *Nano Lett.*, **5**, 1569 (2005); <https://doi.org/10.1021/nl050928v>.
- G. Braun, I. Pavel, A.R. Morrill, D.S. Seferos, G.C. Bazan, N.O. Reich and M. Moskovits, *J. Am. Chem. Soc.*, **129**, 7760 (2007); <https://doi.org/10.1021/ja072533e>.
- T. Shegai, Z. Li, T. Dadoosh, Z. Zhang, H.X. Xu and G. Haran, *Proc. Natl. Acad. Sci. USA*, **105**, 16448 (2008); <https://doi.org/10.1073/pnas.0808365105>.
- Y. Saito, J.J. Wang, D.A. Smith and D.N. Batchelder, *Langmuir*, **18**, 2959 (2002); <https://doi.org/10.1021/la011554y>.
- L.T. Hansen, A. Kühle, A.H. Sørensen, J. Bohr and P.E. Lindelof, *Nanotechnology*, **9**, 337 (1998); <https://doi.org/10.1088/0957-4484/9/4/006>.
- H. Ogura and N. Takahashi, *Progr. Electromag. Res.*, **14**, 89 (1996).
- K. Oikawa, H. Kim, N. Watanabe, M. Shigeno, Y. Shirakawabe and K. Yasuda, *Ultramicroscopy*, **107**, 1061 (2007); <https://doi.org/10.1016/j.ultramic.2007.03.011>.
- P. Klapetek, I. Ohlidal, D. Franta, A. Montaigne-Ramil, A. Bonanni, D. Stifter and H. Sitter, *Acta Phys. Slovaca*, **53**, 223 (2003).
- S.K. Shailesh, B. Tiwari, K. Yadav and D. Prakash, *Int. J. Metallurg. Mater. Sci. Eng.*, **3**, 13 (2013).
- S.K. Shailesh, A.K. Roy and B. Tiwari, *Mechan. Manufact.*, **2**, 14 (2014); <https://doi.org/10.7763/IJMMM.2014.V2.89>.
- R.J. Bandaranayake, G.W. Wen, J.Y. Lin, H.X. Jiang and C.M. Sorensen, *Appl. Phys. Lett.*, **67**, 831 (1995); <https://doi.org/10.1063/1.115458>.
- V. Singh and P. Chauhan, *J. Phys. Chem. Solids*, **70**, 1074 (2009); <https://doi.org/10.1016/j.jpcs.2009.05.024>.
- A.W. Stevenson, M. Milanko and Z. Barnea, *Acta Crystallogr.*, **40**, 521 (1984); <https://doi.org/10.1107/S0108768184002639>.
- J.E. Crowell, E.L. Garfunkel and G.A. Somorjai, *Surf. Sci.*, **121**, 303 (1982); [https://doi.org/10.1016/0039-6028\(82\)90045-0](https://doi.org/10.1016/0039-6028(82)90045-0).
- E. Giamello, A. Ferrero, S. Coluccia and A. Zecchina, *J. Phys. Chem.*, **95**, 9385 (1991); <https://doi.org/10.1021/j100176a064>.